Making Sense of Inter-Signal Corrections

Accounting for GPS Satellite Calibration Parameters in Legacy and Modernized Ionosphere Correction Algorithms

Lockheed Martin

Because satellite designers cannot precisely eliminate small variations in delays among the various signal paths within the spacecraft, GPS signals don't emerge from the satellite antennas at exactly the same time or from the same location. If not accounted for, these delay offsets would produce navigation fix errors for GPS users. In this article, the authors derive and explain the modernized ionosphere dual- and single-frequency correction algorithms that will resolve these inter-signal variations. They also explain how to modernize any new algorithm, how a single ephemeris models the satellite location when each L-band signal may have separate departure points, and why that one ephemeris might point to a location behind the satellite.

InsideGNSS

AVRAM TETEWSKY
CHARLES STARK DRAPER LABORATORY

JEFFRY ROSS
THE MITRE CORPORATION

ARNOLD SOLTZ, NORMAN VAUGHN, JAN ANSZPERGER, CHRIS O'BRIEN, DAVE GRAHAM, DOUG CRAIG, AND JEFF LOZOW
CHARLES STARK DRAPER LABORATORY

The current version of the master GPS Interface Specification document (IS-GPS-200 Rev D March 2006) contains a new dual-frequency ionosphere correction algorithm that is to be used with the modernized GPS space vehicles (SVs) and their next-generation modernized GPS signals.

The Block IIR-M satellites add the new L2C, L1M, and L2M signals on the existing L-band carriers. The Block IIF will also transmit these signals as well as a new L5 signal on the recently established L5 carrier.

Signals/ranging/modulation codes all refer to the various GPS broadcast waveforms that can be present on the L1, L2, or L5 carriers. These codes perform three functions: code division multiple access (CDMA), processing/anti-jam gain, and indication of transmission time by providing each chip a unique time-tag.

The "new" algorithm, which we refer to as "the modernized ionosphere-free pseudorange algorithm," contains a mix of new parameters, inter-signal corrections (ISCs), and the legacy scaled group delay differential parameter T_{GD}. This article describes why a new algorithm is needed, and how the new and old parameters are combined.

With the U.S. Air Force set to begin broadcasting this fall the first of the new CNAV navigation messages on the L2 civil signal transmitted by the Block IIR-M satellites, an understanding of these issues will be important for GPS receiver designers, GNSS signal simulator manufacturers, and end users who require high-precision results from their GPS equipment.

In our presentation, we will first derive the new algorithm by using IS-GPS-200's definition of delay error to model the GPS satellite equipment delays. Then, working through the various paragraphs on how to perform single- and dual-fre-

quency corrections, we can reconstruct the new equations by analyzing the modernized SV model.

Having this modernized model allows one to also derive new results, such as a modernized version of the popular alternative ionosphere correction algorithm — the ionosphere pseudorange difference algorithm and understand why the new algorithm offers a more accurate correction.

Background

Terrestrial users can experience between 3 to 30 meters of ionospheric ranging error due to the effects of phenomena encountered by signals propagating through the atmosphere. At L-band frequencies for a nominal ionosphere, the measured ionosphere range is reasonably modeled as an error that is inversely proportional to the square of the carrier frequency. If no other significant frequency-dependent errors exist, two ranging measurements on different L-band carrier frequencies allow the ionosphere error to be eliminated.

In general, until now only Department of Defense (DoD) receivers that track both the L1 P(Y) and the L2 P(Y) signals could make such a correction. (Some civilian receivers can track the DoD P(Y) code without a crypto key when the signal to noise ratio is sufficiently "high.")

With modernized GPS, however, civilian users will finally have access to a second frequency, the new L2C and/or L5 signals. For DoD users, the new L1M and L2M military signals will provide better cryptography as well as improved accuracy. Moreover, because a pair of M codes will reside on different carriers, dual-frequency ionosphere corrections capability can be maintained on modernized GPS military user equipment.

Because we cannot precisely eliminate small variations in SV equipment delays among the various signal paths within the satellite, these new signals — as well as the legacy signals — don't *exactly* emerge from the satellite antenna at the same time or from the same location. If not accounted for, these delay offsets would produce GPS navigation fix errors for dual- and single-frequency users.

Consequently, IS-GPS-200 provides one ISC for each signal on each L-band. So, a Block IIRM SV with L1 CA, L1P(Y), L1M, L2C, L2P(Y), and L2M, has six ISCs. A GPS follow-on Block IIF satellite that also includes L5I and L5Q (in phase and in quadrature signals, respectively) will have two additional ISCs. The legacy T_{GD} parameter is really the ISC parameter for L2P(Y) scaled by a constant, which we will discuss later.

We will use the following subscript notation when a pair of L-band measurements is being discussed: Li,x will denote one carrier frequency with signal x, and Lj,z will be used for the second L-band carrier frequency and the signals on that carrier. So for L1, Li=L1, and x=CA, P(Y), or M codes. For L2, Lj=L2, and z=L2C, P(Y), or M. For L5, Lj=L5, and z=L5I or L5Q.

In all of the dual frequency correction algorithms, IS-GPS-200 and IS-GPS-705 use the symbol γ_{ij} to represent the ratio of $(f_{Li}/f_{Lj})^2$ of the L-band carrier frequencies squared. If γ is not subscripted, one can assume that it is γ_{12}.

To understand where the small SV equipment–delay errors

come from, consider putting a picture to the words in paragraph 3.3.1.7 of IS-GPS-200 in order to build up a model of the modernized SV as shown in **Figure 1**.

According to paragraph 3.3.1.7, the SV-equipment group delay for each signal is the amount of time it takes the signal to start out from the common clock, travel through each code generator, modulator, transmitter, tri- or quadraplexor, and finally emerge from the satellite's antenna. Thus, the total delay consists of an electrical portion and an antenna portion.

Note that the SV antenna is effectively a two-element array, made up of an inner-ring that produces a broader beam and an outer ring that produces a narrower beam. As discussed in the articles by C. Choi and by G. Mader and F. Czopek listed in the Additional Resources section near the end of this article, the two rings are effectively phased 180 degrees apart so that the narrower beam is subtracted from the wider beam. As a result, the power across the surface of the Earth over the 13-degree half angle of the transmitted signal is approximately constant.

Because the SV antenna is an array, it can have gain, phase, and group delay variations across the beam, although for a properly designed antenna array, any angular variations of delay and phase would be small compared to the total signal-in-space (SIS) error budget. Choi's article notes the distinct locations of the phase centers for each L-band — all signals within an L-band sharing the same phase center, but it does not discuss the group delay characteristics of the SV antenna, nor does it discuss the possibility that each L-band signal may have its own distinct group delay center.

As noted earlier, $ISC_{Li,x}$ is the difference of the transit delay through the SV (including antenna) for L1P(Y) minus the transit delay for the xth or z^{th} signal on the Li or Lj carrier. (It is important to point out that the ISC values, one for each signal, are not affected by the common clock error modeled by a second order polynomial with the coefficients a_{f0}, a_{f1}, and a_{f2} broadcast in subframe 1, as noted in the center of Figure 1, because this error is common to all signals and won't contribute to delay differences.)

The ISC values may age with time or change when redundant components are swapped in as the satellite ages. Each satellite has its own set of ISC values. The legacy parameter T_{GD} is really $ISC_{L2P(Y)}$ scaled by (1-γ).

The ISCs for civil users are broadcast in Message #30 of the CNAV dataset, and the M-code ISCs will be present in the MNAV dataset. The values are based on contractor-measured data. For T_{GD}, on-orbit data is also used, as discussed in the article by B. Wilson et alia listed in Additional Resources.

Problem and Simplified Solution

In this section, we mathematically state our problem and provide a simplified derivation of the legacy versus modernized ionosphere-free pseudorange algorithms by building up a pseudorange error model that properly accounts for SV equipment delays consistent with the IS-GPS-200 ISC parameters, but without delving into the detailed IS-GPS-200 notation.
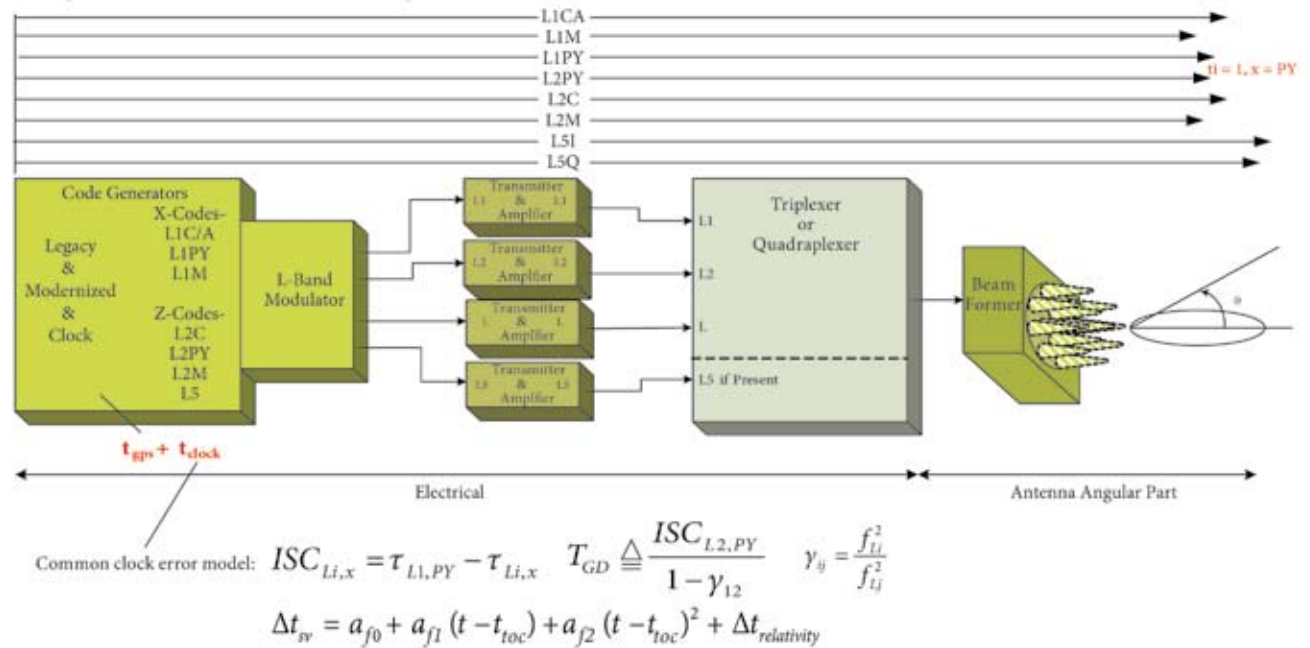
FIGURE 1 Pictorial Summary of SV equipment delay. IS-GPS-200, section 3.3.1.7 states, "Equipment group delay: delay between the signal radiated output of a specific SV (measured at the antenna phase center) and the output of that SV's on-board frequency source" We contend that antenna group delay center per L-band per signal is the precise metric to use for each delay, but later we will show that the SV is made to operate as if there is a single ephemeris and single emanation point.

We should note that, strictly speaking, IS-GPS-200 defines the ISCs in terms of time-tag differences, not delay differences, and it takes a substantial amount of effort and verbiage to prove that the delay notation we use is equivalent to the time-tag notation used in reference 1.

Also of interest is the fact that, historically, IS-GPS-200 was written for engineers who were building entire GPS receivers; thus, many of the compensation algorithms are stated in terms of the delay lock loop's code phase read-out of the time of transmission as measured by the receiver. Only later is the final pseudorange formed as the user time minus time of transmission scaled by the speed of light, *c*.

For our full derivation of the new algorithm with all of the exhaustive details, readers can download an extended version of this article from the *Inside GNSS* website <www.insidegnss.com>.

Although IS-GPS-200 can be tedious to read, a tremendous number of insights can be gleamed from it. (As an aside, it would be nice if a team of authors could write a companion document to IS-GPS-200 that describes why certain decisions were made, and to provide derivations, so that valuable knowledge will not be lost as people retire.)

Problem Statement

Most readers are familiar with the legacy ionosphere-free dual-frequency correction algorithm for the L1P(Y) and L2P(Y) codes from IS-GPS-200, paragraph 20.3.3.3.3, as shown on the left side of **Figure 2**.

Legacy vs. Modernized Dual Frequency Corrections

| Start with a pair of L_i and L_j pseudoranges: | $\rho_{m_{Li,x}} = \rho_{LOS} + R_{trop} + \dfrac{A}{f_{Li}^2} + ... \qquad \rho_{m_{Lj,x}} = \rho_{LOS} + R_{trop} + \dfrac{A}{f_{Lj}^2} + ...$ | |

• Legacy:	• Modernized: reduces to legacy:
$\rho_{iono\_free} =$ $\dfrac{\rho_{mL2,PY} - \gamma \cdot \rho_{mL1,PY}}{1-\gamma}$	$\rho_{iono\_free} =$ $\dfrac{\rho_{mLj,z} - \gamma_{ij} \cdot \rho_{mL_{i,x}} + c \cdot [ISC_{Lj,z} - \gamma_{ij} \cdot ISC_{Li,x}]}{1-\gamma_{ij}} - c \cdot T_{GD}$

| Get an ionosphere free pseudorange: | $\rho_{iono\_free} = \rho_{LOS} + R_{trop} + ..$ | $\sigma_{pos} = 1.5 \cdot GDOP \cdot 1.7 \cdot \sigma_{ISC}$ |

Where: $\gamma = \dfrac{f_{L1}^2}{f_{L2}^2}$; note: $\gamma_{12} = \dfrac{f_{L1}^2}{f_{L2}^2}, \gamma_{15} = \dfrac{f_{L1}^2}{f_{L5}^2}, \gamma_{x} = \dfrac{f_{Li}^2}{f_{Lj}^2} \qquad ISC_{Li,x} = \tau_{L1,PY} - \tau_{Li,x} \qquad T_{GD} \triangleq \dfrac{ISC_{L2,PY}}{1-\gamma} = \dfrac{\tau_{L1,PY} - \tau_{L2,PY}}{1-\gamma}$

FIGURE 2 Legacy versus modernized ionosphere-free dual-frequency algorithms. Note that T_{GD} is needed even for L1/L5 correction!

Given two pseudorange measurements $\rho_{m_{Li,PY}}$ (in meters) at two distinct L-band frequencies f_{Li} and f_{Lj}, with a true line-of-sight term, ρ_{LOS}, a common frequency-independent troposphere error, R_{trop}, a frequency-dependent $\frac{A}{f_L^2}$ ionosphere term, and some possible measurement noise, in order to eliminate a nominal $\frac{A}{f_L^2}$ meter ionospheric ranging error IS-GPS-200 (paragraph 20.3.3.3.3) instructs the user to form an ionosphere-free pseudorange as:

$$\rho_{iono\_free} = \frac{\rho_{mL2,PY} - \gamma \cdot \rho_{mL1,PY}}{1-\gamma} = \rho_{LOS} + R_{trop} + ... \qquad (1)$$

where

$\gamma = \dfrac{f_{L1}^2}{f_{L2}^2}$ (and in the future, $\gamma_{ij} = \dfrac{f_{Li}^2}{f_{Lj}^2}$ to allow for L1/L2 or L1/L5.) Assume L1/L2 and the pseudo-range measurements in the form of

$$\rho_{m_{L1,PY}} = \rho_{LOS} + R_{trop} + \frac{A}{f_{L1}^2} + \dots \text{ and } \rho_{m_{L2,PY}} = \rho_{LOS} + R_{trop} + \frac{A}{f_{L2}^2} + \dots$$

With some simple algebra, one can see that multiplication by the ratio of the frequency-squared term eliminates the ionosphere term, leaving an ionosphere free measurement.

In Search of the Modernized Ionosphere–Free Pseudorange Equation

Although IS-GPS-200 notes in paragraph 20.3.3.3.2 that some type of SV equipment–delay compensation has been done by adjusting the clock offset coefficient a_{f0}, it has not been explicitly modeled in any of the popular GPS textbooks. However, the "rev D" version of IS-GPS-200 and IS-GPS-705 provide the modernized ionosphere-free pseudorange equation that accounts for hardware delay errors for either L1/L2 or L1/L5 measurement pairs.

Given that the xth signal on the Li^{th} L-band in a modernized GPS SV has a unique hardware delay offset, $\tau_{Li,x}$ seconds — or, by scaling by the speed of light c meters/second, that is $+c \cdot \tau_{Li,x}$ meters — the equation is applied when one forms the ionosphere-free pseudorange using measurements from different signals on different L-band carriers, using either an L1/L2 or L1/L5 measurement. This equation, which can also be seen on the right-hand side of Figure 2, is as follows:

$$\rho_{iono\_free} = \frac{\rho_{m_{Lj,z}} - \gamma_{ij} \cdot \rho_{m_{Li,x}} + c \cdot [ISC_{Lj,z} - \gamma_{ij} \cdot ISC_{Li,x}]}{1 - \gamma_{ij}} - c \cdot T_{GD} \quad \textbf{(2)}$$

In this new equation, note that all of the hardware errors seem to be accounted for by differential effects, because the only parameters in this equation are the inter-signal corrections, which are defined as the delay difference relative to the SV delay error of L1 P(Y) code, i.e., $ISC_{Li,x} = \tau_{L1,PY} - \tau_{Li,x}$. Even the legacy parameter T_{GD} is defined as: $T_{GD} \triangleq ISC_{L2,PY} / (1 - \gamma)$ and is referenced to L1P(Y).

On the surface, it appears that the L1P(Y) is the master reference code to which all other codes are aligned. We will soon see that this not the case.

Single frequency users who obtain ionosphere compensation from other sources are familiar with the legacy compensation equations. Note that the compensation equations as written in IS-GPS-200 are expressed in terms of raw code phase measurements prior to forming pseudoranges.

Figure 3 summarizes the key pseudorange equation followed by the legacy algorithm on the left, and the modernized algorithm on the right.

As defined in IS-GPS-200, a pseudorange is fundamentally expressed as the difference between user time in the receiver, t_u, and the time of transmission from the SV as measured by the user at their receiver, $t_{sv\_Li,x}$ (note these terms in the equation at the top of Figure 3).

Legacy vs. Modernized Single Frequency Corrections

$$\rho_{m_{Li,x}} \triangleq c \cdot (t_u - t_{sv\_Li,x}) \qquad t_{sv\_Li,x} = t_{sv\_uncompensated} - (\Delta t_{sv})_{Li,x}$$

Legacy: IS-GPS-200, 20.3.3.3.2. This correction term is only for the benefit of "single-frequency" (L1 P/Y or L2 P/Y) users. $(\Delta t_{sv})_{L1PY} = \Delta t_{sv} - T_{GD}$ $(\Delta t_{sv})_{L2PY} = \Delta t_{sv} - \gamma T_{GD}$	Modernized: IS-GPS-200, 30.3.3.3.1.1.1 For maximum accuracy, the single-frequency L1 C/A user must use the correction terms to make further modifications to the code phase offset in paragraph 20.3.3.3.1 with the equation: $(\Delta t_{sv})_{Li,x} = \Delta t_{sv} - T_{GD} + ISC_{Li,x}$

where: $\Delta t_{sv} = a_{f0} + a_{f1}(t - t_{oc}) + a_{f2}(t - t_{oc})^2 + \Delta t_{relativity}$ removes common clock error, and $(\Delta t_{sv})_{Li,x}$ is applied to final prange

FIGURE 3 **Legacy versus modernized single-frequency algorithms. The legacy correction term is required by the fact that the SV clock offset estimates reflected in the a_{f0} clock correction coefficient are based on the effective PRN code phase, as apparent with dual-frequency — L1 P(Y) and L2 P(Y) — ionospheric corrections. The modernized correction terms, T_{GD}, $ISC_{L1C/A}$ and ISC_{L2C}, account for the effect of SV group delay differential between L1 P(Y) and L2 P(Y), L1 P(Y) and L1 C/A, and between L1 P(Y) and L2 C, respectively.**

Any corrections made to the measured time of transmission are essentially corrections to the measured pseudorange with a sign flip and scaling by the speed of light c to convert time into distance. Without getting bogged down in details, the SV transmission time measurement is corrupted by a common clock term and SV signal–specific equipment delays, unique to each SV that are contained in the ISCs.

As indicated in Figure 3, all users must first apply the common clock polynomial correction using a second order polynomial with coefficients a_{f0}, a_{f1}, and a_{f2} to the raw/uncompensated transmission time measurement. (The transmission time measurements are the raw code phase measurements, which are extracted from the prompt-tap numerically controlled oscillator code phase of the delay lock loop).

For legacy L1P(Y)/L2P(Y) users, the left side of Figure 3 indicates that L1P(Y) and L2P(Y) single-frequency users are to remove T_{GD} from the L1P(Y) code phase measurement and $\gamma \cdot T_{GD}$ from the L2P(Y) code phase measurement. These corrections are necessary due to a special compensation that is embedded in the a_{f0} term to allow dual-frequency L1P(Y)-L2P(Y) receivers to use the legacy ionosphere-free pseudorange algorithm.

The right side of Figure 3 summarizes the modernized single-frequency corrections generalized for any signal, which involves removing T_{GD} - $ISC_{Li,x}$ from the xth signal on the Li^{th} frequency code phase measurement.

As noted earlier, IS-GPS-200 states that a special compensation has been added to the a_{f0} term, but it does not explicitly state or derive the actual term. Thus, our goals are to:
1. Derive: ,

$$\rho_{iono\_free} = \frac{\rho_{m_{Lj,z}} - \gamma_{ij} \cdot \rho_{m_{Li,x}} + c \cdot [ISC_{Lj,z} - \gamma_{ij} \cdot ISC_{Li,x}]}{1 - \gamma_{ij}} - c \cdot T_{GD},$$

the modernized ionosphere-free dual-frequency pseudorange equation in section 30.3.3.3.1.1.2 of IS-GPS-200. .

FIGURE 4 Finding the implicit L1P(Y)/L2P(Y) error term

2. Compare the modernized ionosphere-free dual-frequency pseudorange equation to the legacy equation

$$\rho_{iono\_free} = \frac{\rho_{m_{L2,PY}} - \gamma \cdot \rho_{m_{L1,PY}}}{1-\gamma}$$

and explain why the L1P(Y) and L2P(Y) hardware delay parameters don't show up.

3. Derive all of the various single and dual-frequency compensation options presented in the Rev D or later IS-GPS-200 releases, sections 20.3.3.3.3.2 and 20.3.3.3.3.1, and 30.3.3.3.1.1.1.

4. Explain some of its curious properties of the modernized correction algorithm, such as why the legacy L1/L2 parameter T_{GD} comes into to play even when an L1/L5 correction is done.

5. Using our SV transmission model, derive a modernized version of the popular alternative ionosphere correction algorithm — the ionosphere difference algorithm — that can potentially deliver better performance when measurement noise is present when the ionosphere term is slowly varying.

Simplified IS–GPS–200 Modernized Ionosphere Algorithm Derivations

Our first task is to find the hidden term that is placed in the constant term (a_{f0}) of the common clock model. We will use the following coloring scheme to assist in the analysis when two measurements from different frequency L bands are combined: terms that are common to both measurements are blue, terms that vary exactly as $1/f_{Li}^2$ are purple, and terms that are different on both measurements but don't vary inversely with frequency squared are red. (Red is also used for hardware delays that might be the same on each channel, but affect the pseudorange compensation.)

Consider the following simplified model of the measured pseudoranges. Starting at the satellite, the uncompensated pseudorange measurement for any signal 'x' on the ith L-band carrier 'Li', $\rho_{um_{Li,x}}$, will consist of the following elements:

• an SV clock error that will be common to all signals, which after scaling by the speed of light c would be $-c \cdot t_{clock\_in\_SV}$ in meters

• a signal and carrier unique hardware delay, $+c \cdot \tau_{Li,x}$

• the common true line-of-sight (LOS) range, R_{LOS}

• an ionosphere error term that has a inverse square frequency dependence of $\frac{A}{f_{Li}^2}$ meters

• a troposphere term that is independent of frequency, R_{trop}

• the user's GPS receiver's clock bias of $c \cdot t_{bias}$ in meters.

Note that the LOS pseudorange is the sum of the LOS range and the receiver's clock bias, or $\rho_{LOS} = c \cdot t_{bias} + R_{LOS}$. Because the common clock term, $-c \cdot t_{clock\_in\_SV}$, is eliminated by the broadcast clock coefficients, for now we will not track that term in detail.

Thus, incorporating the assumed sign convention, a simplified pseudorange model that includes SV equipment delays is shown in **Figure 4**.

Starting with a simplified pseudorange error model that includes the compensation for the common clock, but not any L1L2P(Y) precompensation of a_{f0} by ground control(denoted with a "*"), the pseudorange model would be:

$$\rho_{m^*_{Li,x}} = \rho_{LOS} + c \cdot \tau_{Li,x} + \frac{A}{f_{Li}^2} + R_{trop} \quad (3)$$

For L1P(Y) and L2P(Y) signals, they are:

$$\rho_{m^*_{L1,PY}} = \rho_{LOS} + c \cdot \tau_{L1,PY} + \frac{A}{f_{L1}^2} + R_{trop} \quad (4)$$

$$\rho_{m^*_{L2,PY}} = \rho_{LOS} + c \cdot \tau_{L2,PY} + \frac{A}{f_{L2}^2} + R_{trop} \quad (5)$$

When inserting the foregoing equations into the ionosphere free pseudorange algorithm,

$$\rho_{iono\_free} = \frac{\rho_{m_{L2,z}} - \gamma \cdot \rho_{m_{L1,x}}}{1-\gamma} \quad (6)$$

the following two simple identities should be noted for weak plasma ionospheres that vary as

$$R_{iono\_L1} - R_{iono\_L2} = \frac{A}{f_{L1}^2} - \frac{A}{f_{L2}^2} = \frac{A}{f_{L1}^2}(1 - \frac{f_{L1}^2}{f_{L2}^2}) = \frac{A}{f_{L1}^2}(1-\gamma) \quad (7)$$

with $\gamma = \frac{f_{L1}^2}{f_{L2}^2}$

Next, multiplying the L1 carrier frequency ionosphere error by γ produces the L2 ionosphere error,

$$\gamma \cdot R_{iono\_L1} = \gamma \frac{A}{f_{L1}^2} = \frac{A}{f_{L2}^2} = R_{iono\_L2} \quad (8)$$

Further Steps in Deriving the Ionosphere Correction Algorithm

From the two previous equations, one can see that, with two simultaneous pseudorange measurements from different L-band carrier frequencies, equation (6)

$$\rho_{iono\_free} = \frac{\rho_{m_{L2,z}} - \gamma \cdot \rho_{m_{L1,x}}}{1-\gamma}$$

has the following properties:

1. Any term in each pseudorange measurement that is the same for both measurements, such as the LOS pseudorange, ρ_{LOS}, or troposphere error term, R_{trop}, will be preserved.

2. Any error terms that vary exactly as $1/f_{Li}^2$, such as the weak ionosphere errors of $\frac{A}{f_{Li}^2}$ (in meters), will be eliminated.

3. Any error terms that are different on both L-band carrier frequencies, such as the SV hardware delay errors $\tau_{Li,x}$, will remain and show up as a linear combination of the individual terms in each measurement.

Although this last point seems like a new error source, it has always been present. The hardware delay errors were possible to ignore because they were automatically compensated for when using L1P(Y) and L2P(Y), but with the new signals these delays resurface because the compensation only worked for L1P(Y) and L2P(Y).

Substituting the model for the uncompensated pseudorange measurements reflected in equations (3–5) into the ionosphere-free pseudorange expression (6), using the identities (7), and the three listed properties, produces the following:

$$\rho_{iono\_free\_L1L2PY} = \frac{\rho_{m_{L2,PY}} - \gamma \bullet \rho_{m_{L1,PY}}}{1-\gamma} \text{ and } \gamma = \frac{f_{L1}^2}{f_{L2}^2}$$

$$\rho_{iono\_free\_L1L2PY} = \frac{(\rho_{LOS} + c \bullet \tau_{L2,PY} + \frac{A}{f_{L2}^2} + R_{trop}) - \gamma \bullet (\rho_{LOS} + c \bullet \tau_{L1,PY} + \frac{A}{f_{L1}^2} + R_{trop})}{1-\gamma}$$

note: $\dfrac{A}{f_{L2}^2} = \gamma \bullet \dfrac{A}{f_{L1}^2}$

$$\rho_{iono\_free\_L1L2PY} = \rho_{LOS} + R_{trop} + c \bullet \frac{\tau_{L2,PY} - \gamma \bullet \tau_{L1,PY}}{1-\gamma}$$

The inverse frequency-square ionosphere terms, $\frac{A}{f_{Li}^2}$, are removed, but signal-unique hardware delay error terms such as $\tau_{Li,x}$ remain. This is the term most people don't recognize because it has been removed from view for L1P(Y) and L2P(Y) users.

We will show in a later section, "Interpreting the Modernized SV Model and Ionosphere Correction Equations," that the signal-unique delay error term in (9),

$$\frac{\tau_{L2,z} - \gamma \bullet \tau_{L1,x}}{1-\gamma},$$

has a special meaning when the L1P(Y) and L2P(Y) codes are used. We will also define a term, the Y-code ionosphere-free delay center for L1P(Y) and L2P(Y), or T_{YIFDC}, as

$$T_{YIFDC} \triangleq \frac{\tau_{L2,PY} - \gamma \bullet \tau_{L1,PY}}{1-\gamma} \qquad (10)$$

and explain how it is used, how it affects users regardless of what signals are being used, and give it a physical interpretation.

For now, consider equation (10) as an extra delay offset for a "effective" ranging signal made up of a linear combination of L1P(Y) and L2P(Y), that is, the ionosphere free L1P(Y)-L2P(Y) signal. Given that an error term appears in equation (9) that is a mixture of absolute delay parameters $\tau_{Li,x}$, which are physically

---

Simplified Derivation: The a_{f0} on all signals

- **Assume** a_{f0} contains: $\dfrac{\tau_{L2,PY} - \gamma \bullet \tau_{L1,PY}}{1-\gamma}$ because ICD says any L1PY/L2PY delay errors are automatically removed

- **Then above term is subtracted off from all other measurements**
  - With simple algebra, we can show that the remainder is now an ISC term and a T_{GD} term.

$$\rho_{m_{Li,x}} = \rho_{LOS} + c \bullet (\tau_{Li,x} - \frac{\tau_{L2,PY} - \gamma \bullet \tau_{L1,PY}}{1-\gamma}) + \frac{A}{f_{Li}^2} + R_{trop}$$

NOTE: $\tau_{Li,x} - \dfrac{\tau_{L2,PY} - \gamma \bullet \tau_{L1,PY}}{1-\gamma} = -ISC_{Li,x} + T_{GD}$

and 30.3.3.3.1.1.1 confirms that $-ISC_{Li,x} + T_{GD}$ is the remaining error if you are a single frequency user

Thus: $\rho_{m_{Li,x}} = \rho_{LOS} + c \bullet \tau_{Li,x} + \dfrac{A}{f_{Li}^2} + R_{trop}$ becomes

$$\rho_{m_{Li,x}} = \rho_{LOS} + c \bullet (T_{GD} - ISC_{Li,x}) + \frac{A}{f_{Li}^2} + R_{trop} \text{ when } a_{f0} \text{ absorbs } \frac{\tau_{L2,PY} - \gamma \bullet \tau_{L1,PY}}{1-\gamma}$$

FIGURE 5 **The effect of moving the L1P(Y)–L2P(Y) error into a_{f0}**

---

difficult if not impossible to measure, one needs to eliminate this term, at least for the L1P(Y)-L2P(Y) pair of signals.

To accomplish this, consider the following simplified argument (which will be formally proven in the full on-line article). If one were to use the ionosphere-free pseudorange as truth, making it the master reference code to calculate the clock polynomial coefficients, this would in effect subtract this term (9) from the full range and from each signal unique delay $\tau_{Li,x}$. Thus, if the ionosphere free pseudorange using a combination of L1P(Y) and L2P(Y) were the master reference code, the term

$$\frac{\tau_{L2,PY} - \gamma \bullet \tau_{L1,PY}}{1-\gamma}$$

would be subtracted off from any measurement model, equations (3 through 5).

Given that this term looks like a delay offset, it would be built into the a_{f0} clock polynomial coefficient time offset. Section 20.3.3.3.3.1 of IS-GPS-200 notes that the clock polynomial has been adjusted so that L1P(Y) and L2P(Y) users will not see any dual-frequency correction errors.

The offset term (10), $\dfrac{\tau_{L2,PY} - \gamma \bullet \tau_{L1,PY}}{1-\gamma}$

when differenced with any one of the absolute delay terms, $\tau_{Li,x}$, will produce a new term that is a function of only measureable delay differences and, in fact, will consist of terms that are broadcast by ground control. This is summarized in **Figure 5**.

Final Approach to the Equation

The following expressions will be extremely important in this article and will later be recognized as the modernized single-frequency compensation terms in IS-GPS-200.

$$\frac{\tau_{L2PY} - \gamma \tau_{L1PY}}{1-\gamma} - \tau_{Li,x} = T_{YIFDC} - \tau_{Li,x} = -T_{GD} + ISC_{Li,x} \qquad (11)$$

Equation (11) is derived in an appendix that will be presented in the extended version of the article posted online. Note that strictly speaking, the T_{GD} term is independent of frequency and common to both measurements. However, because the pair of terms together makes up the SV signal specific equipment errors, we have left both terms in red.

From **Figure 6**, we conclude that when the ionosphere free L1P(Y)/L2P(Y) pseudorange is used as the truth model to assist in fitting the clock polynomial, when the user corrects for the common clock error using the modified second order polynomial, with coefficients a_{f0}, a_{f1}, a_{f2}, that contains equation (10) built into the a_{f0} term, the effective pseudorange error model for all signals becomes equation (12):

$$\rho_{m_{Li,x}} = \rho_{LOS} + c \bullet (T_{GD} - ISC_{Li,x}) + \frac{A}{f_{Li}^2} + R_{trop} \tag{12}$$

Notice that we have removed the * in our designation because the L1/L2P(Y) pre-compensation to a_{f0} has been applied by ground control. Using (12) as the model of the pseudorange, when (12) is inserted into the ionosphere free pseudorange equation as shown in Figure 6, one can identify the desired blue terms, place them on the left side, and solve for them as a function of all other terms.

Thus, we insert:

$$\rho_{m_{Li,x}} = \rho_{LOS} + c \bullet (T_{GD} - ISC_{Li,x}) + \frac{A}{f_{Li}^2} + R_{trop} \tag{13}$$

$$\rho_{m_{Lj,z}} = \rho_{LOS} + c \bullet (T_{GD} - ISC_{Lj,z}) + \frac{A}{f_{Lj}^2} + R_{trop} \tag{14}$$

into

$$\rho_{iono\_free} = \frac{\rho_{m_{L2,z}} - \gamma \bullet \rho_{m_{L1,x}}}{1 - \gamma} \tag{6}$$

and it becomes

$$\frac{\rho_{m_{Lj,z}} - \gamma_{ij} \bullet \rho_{m_{Li,x}}}{1 - \gamma_{ij}} =$$

$$\frac{(\rho_{LOS} + c \bullet (T_{GD} - ISC_{Lj,z}) + \frac{A}{f_{Lj}^2} + R_{trop}) - \gamma_{ij} \bullet (\rho_{LOS} + c \bullet (T_{GD} - ISC_{Li,x}) + \frac{A}{f_{Li}^2} + R_{trop})}{1 - \gamma_{ij}} \tag{15}$$

Then, if we collect the desired blue terms and place them on the left side of the equation, noting that all of the purple terms add to zero, after collecting all other terms and placing them on the right hand side the final expression that remains is:

$$\rho_{LOS} + R_{trop} = \frac{\rho_{m_{Lj,z}} - \gamma_{ij} \bullet \rho_{m_{Li,x}} + c \bullet (ISC_{Lj,z} - \gamma_{ij} \bullet ISC_{Li,x})}{1 - \gamma_{ij}} - c \bullet T_{GD} \tag{16}$$

Thus, equation (16) is recognized as the modernized ionosphere-free pseudorange equation. In **Figure 7**, one can check for backward compatibility to see that (16) reduces to (6) when one is only using L1P(Y) and L2P(Y).

One can also perform a second backward-compatibility check on the single-frequency compensations, as shown in **Figure 8**.

Simplified Derivation: Derive Modernized Iono Free Equation

- If (T_{GD}-$ISC_{Li,x}$) is the error, then

$$\rho_{m_{Li,x}} = \rho_{LOS} + c \bullet (T_{GD} - ISC_{Li,x}) + \frac{A}{f_{Li}^2} + R_{trop}$$

$$\rho_{m_{Lj,z}} = \rho_{LOS} + c \bullet (T_{GD} - ISC_{Lj,z}) + \frac{A}{f_{Lj}^2} + R_{trop}$$

Evaluate $\dfrac{\rho_{m_{Li,z}} - \gamma_{ij} \bullet \rho_{m_{Li,x}}}{1 - \gamma_{ij}}$ noting $\gamma_{ij} = \dfrac{f_{Li}^2}{f_{Lj}^2}$ and collect $\rho_{LOS} + R_{trop}$ terms:

$$\frac{\rho_{m_{Li,z}} - \gamma_{ij} \bullet \rho_{m_{Li,x}}}{1 - \gamma_{ij}} = \frac{(\rho_{LOS} + c \bullet (T_{GD} - ISC_{Lj,z}) + \frac{A}{f_{ij}^2} + R_{trop}) - \gamma_{ij} \bullet (\rho_{LOS} + c \bullet (T_{GD} - ISC_{Li,x}) + \frac{A}{f_{Li}^2} + R_{trop})}{1 - \gamma_{ij}}$$

$$\frac{\rho_{m_{Li,z}} - \gamma_{ij} \bullet \rho_{m_{Li,x}}}{1 - \gamma_{ij}} = \rho_{LOS} + R_{trop} + \frac{c \bullet (-ISC_{Lj,z} + \gamma_{ij} \bullet ISC_{Li,x})}{1 - \gamma_{ij}} + c \bullet T_{GD}$$

or $\rho_{LOS} + R_{trop} = \dfrac{\rho_{m_{Lj,z}} - \gamma_{ij} \bullet \rho_{m_{Li,x}} + c \bullet (ISC_{Lj,z} - \gamma_{ij} \bullet ISC_{Li,x})}{1 - \gamma_{ij}} - c \bullet T_{GD}$

FIGURE 6 Modernized ionosphere-free pseudorange derivation using our modernized pseudorange error model

Simplified Derivation: Back Compatibility check #1

$$\rho_{LOS} + R_{trop} = \frac{\rho_{m_{Lj,z}} - \gamma_{ij} \bullet \rho_{m_{Li,x}} + c \bullet (ISC_{Lj,z} - \gamma_{ij} \bullet ISC_{Li,x})}{1 - \gamma_{ij}} - c \bullet T_{GD}$$

$$\rho_{LOS} + R_{trop} = \frac{\rho_{m_{L2,PY}} - \gamma_{12} \bullet \rho_{m_{L1,PY}} + c \bullet (ISC_{L2,PY} - \gamma_{12} \bullet ISC_{L1,PY})}{1 - \gamma_{12}} - c \bullet T_{GD}$$

but: $ISC_{L1,PY} = 0$, $\dfrac{ISC_{L2,PY}}{1 - \gamma_{12}} = T_{GD}$

so $\boxed{\rho_{LOS} + R_{trop} = \dfrac{\rho_{m_{L2,PY}} - \gamma_{12} \bullet \rho_{m_{L1,PY}}}{1 - \gamma_{12}}}$ $\gamma_{ij} = \dfrac{f_{Li}^2}{f_{Lj}^2}$

FIGURE 7 Simplified derivation of backward compatibility check for dual-frequency L1P(Y)/L2P(Y) users. The new IS-GPS-200 dual-frequency ionosphere free pseudorange correction reduces to legacy version for L1P(Y) and L2P(Y).

From Figure 8, it is interesting to note that by shifting the a_{f0} time offset by equation (10), the remaining errors on L1P(Y) and L2P(Y) scale exactly by $1/f_{Li}^2$, which explains why the legacy equations work and why the legacy ionosphere-free pseudorange equation only had to deal with perfect $1/f_{Li}^2$ errors on L1P(Y) and L2P(Y).

An interesting aside leads to a very pleasing rearrangement of the modernized dual-frequency correction algorithm. First, express the single-frequency corrections in IS-GPS-200 (Figures 4 and 8) in terms of a pseudorange. If the model of the uncompensated measured pseudorange after doing the common clock correction is:

$$\rho_{m_{Li,x}} = \rho_{LOS} + c \bullet (T_{GD} - ISC_{Li,x}) + \frac{A}{f_{Li}^2} + R_{trop} \tag{12}$$

then it is clear that to correct the pseudorange for the Li,x[th] signal, one should subtract $c \bullet (T_{GD} - ISC_{Li,x})$ from it (or due to the sign flip, add this to the time of transmission measurement as stated in IS-GPS-200).

One can easily factor the modernized ionospheric pseudo-range equation into a form that shows that each pseudorange is undergoing a single frequency correction, and then being processed for idealized dual frequency measurements as shown below using some trivial algebraic manipulations.

$$\rho_{LOS} + R_{trop} = \frac{\rho_{m_{Lj,z}} - \gamma_{ij} \bullet \rho_{m_{Li,x}} + c \bullet (ISC_{Lj,z} - \gamma_{ij} \bullet ISC_{Li,x})}{1 - \gamma_{ij}} - c \bullet T_{GD}$$

as written in IS-GPS-200

$$\rho_{LOS} + R_{trop} = \frac{\rho_{m_{Lj,z}} - \gamma_{ij} \bullet \rho_{m_{Li,x}} + c \bullet (ISC_{Lj,z} - \gamma_{ij} \bullet ISC_{Li,x})}{1 - \gamma_{ij}} - \frac{c \bullet (1 - \gamma_{ij}) \bullet T_{GD}}{1 - \gamma_{ij}}$$

$$\rho_{LOS} + R_{trop} = \frac{[\rho_{m_{Lj,z}} - c \bullet (T_{GD} - ISC_{Lj,z})] - \gamma_{ij} \bullet [\rho_{m_{Li,x}} - c \bullet (T_{GD} - ISC_{Li,x})]}{1 - \gamma_{ij}}$$

(13) or viewed in terms of single-frequency compensation being applied first to each pseudorange.

When this equation is specialized to P(Y) code, one gets:

$$\rho_{LOS} + R_{trop} = \frac{[\rho_{m_{L2,PY}} - c \bullet (\gamma \bullet T_{GD})] - \gamma \bullet [\rho_{m_{L1,PY}} - c \bullet (T_{GD})]}{1 - \gamma} =$$

$$= \frac{\rho_{m_{L2,PY}} - \gamma \bullet \rho_{m_{L1,PY}}}{1 - \gamma}$$

As noted in the full on-line version of the article, if one always applies the full single-frequency compensation to the pseudoranges, then, one can always use an idealized dual frequency correction algorithm that does not have to account for the SV equipment delays.

Simplified Alternative Algorithm Derivations

We can now use our modernized pseudorange error modeling equations to derive the popular alternative ionosphere difference algorithm. Although the IS-GPS-200 ionosphere-free pseudorange algorithm does the job of removing the ionosphere, it does so at a cost of amplifying any measurement noise due to the $\gamma / (1 - \gamma)$ terms. For the L1/L2 bands, that term is about 1.5 in value.

For most users near the surface of the earth, the ionosphere term is not changing as fast as the line of sight pseudorange; so, if one could isolate the ionosphere error and strip off time-varying pseudorange measurements, it would be possible to time-smooth (low pass filter) the ionosphere term, and then subtract the smoothed ionosphere term from each measurement.

Using our modernized pseudorange error model of equation (12)

$$\rho_{m_{Li,x}} = \rho_{LOS} + c \bullet (T_{GD} - ISC_{Li,x}) + \frac{A}{f_{Li}^2} + R_{trop}$$

One can apply this model to the ionosphere difference algorithm that has been discussed in popular GPS text books as shown in **Figure 9**.

Simplified Derivation: Back Compatibility check #2

Modernized: $(\Delta t_{sv})_{Li,x} = \Delta t_{sv} - T_{GD} + ISC_{Li,x}$

For L1PY: because $ISC_{L1,PY} = 0$

thus: $(\Delta t_{sv})_{L1,PY} = \Delta t_{sv} - T_{GD}$

For L2PY: because $ISC_{L2,PY} = (1 - \gamma_{12})T_{GD}$

thus: $(\Delta t_{sv})_{L2,PY} = (\Delta t_{sv}) - y_{12}T_{GD}$

note: $ISC_{Li,x} = \tau_{L1,PY} - \tau_{L1,x}$, $ISC_{L1,PY} = 0$, $\frac{ISC_{L2,PY}}{1 - \gamma_{12}} = T_{GD}$, $\gamma_{ij} = \frac{f_{Li}^2}{f_{Lj}^2}$

where: $\Delta t_{sv} = a_{f0} + a_{f1}(t - t_{oc}) + a_{f2}(t - t_{oc})^2 + \Delta t_{relativity}$ removes common clock error and applied to final prange

FIGURE 8 Simplified derivation of backward compatibility check for single-frequency L1P(Y)/L2P(Y) users. The new IS-GPS-200 single-frequency compensation reduces down to legacy equation for L1P(Y) and L2P(Y).

Modernized Alternative Algorithms: Ionosphere difference algorithm

Evaluate: $\rho_{m_{Li,x}} - \rho_{m_{Lj,z}}$ and solve for $\frac{A}{f_{Li}^2}$ using new model of pseudo-ranges

$$\rho_{m_{Li,x}} = \rho_{LOS} + c \bullet (T_{GD} - ISC_{Li,x}) + \frac{A}{f_{Li}^2} + R_{trop}$$

$$\rho_{m_{Lj,z}} = \rho_{LOS} + c \bullet (T_{GD} - ISC_{Lj,z}) + \frac{A}{f_{Lj}^2} + R_{trop}$$

and get: $\rho_{m_{Li,x}} - \rho_{m_{Lj,z}} = \frac{A}{f_{Li}^2} - \frac{A}{f_{Lj}^2} - c \bullet (ISC_{Li,x} - ISC_{Lj,z})$

$$\rho_{m_{Li,x}} - \rho_{m_{Lj,z}} = \frac{A}{f_{Li}^2}(1 - \gamma_{ij}) - c \bullet (ISC_{Li,x} - ISC_{Lj,z})$$

Solve for: $\frac{A}{f_{Li}^2} = \frac{\rho_{m_{Li,x}} - \rho_{m_{Lj,z}} + c \bullet (ISC_{Li,x} - ISC_{Lj,z})}{(1 - \gamma_{ij})}$

FIGURE 9 Modernized ionosphere difference algorithm. Ionosphere difference algorithm eliminates any fast-varying but common terms so that smoothing on the remaining ionosphere term can be done, reducing measurement noise effects.

In Figure 9, when one differences the two pseudoranges, the ionosphere term becomes a function of the pseudorange differences and ISC differences that, also viewed in terms of the difference of single-frequency compensated pseudoranges, can be expressed as the following:

$$\frac{A}{f_{Li}^2} = \frac{\rho_{m_{Li,x}} - \rho_{m_{Lj,z}} + c \bullet (ISC_{Li,x} - ISC_{Lj,z})}{(1 - \gamma_{ij})} = \qquad \text{(17)}$$

$$= \frac{[\rho_{m_{Li,x}} - c \bullet (T_{GD} - ISC_{Li,x})] - [\rho_{m_{Lj,z}} - c \bullet (T_{GD} - ISC_{Lj,z})]}{(1 - \gamma_{ij})}$$

If one specializes equation (17) to finding the L1 ionosphere term when using P(Y) code on L1 and L2, it does not reduce down to the legacy equations published in popular text books due to the trailing T_{GD} term,
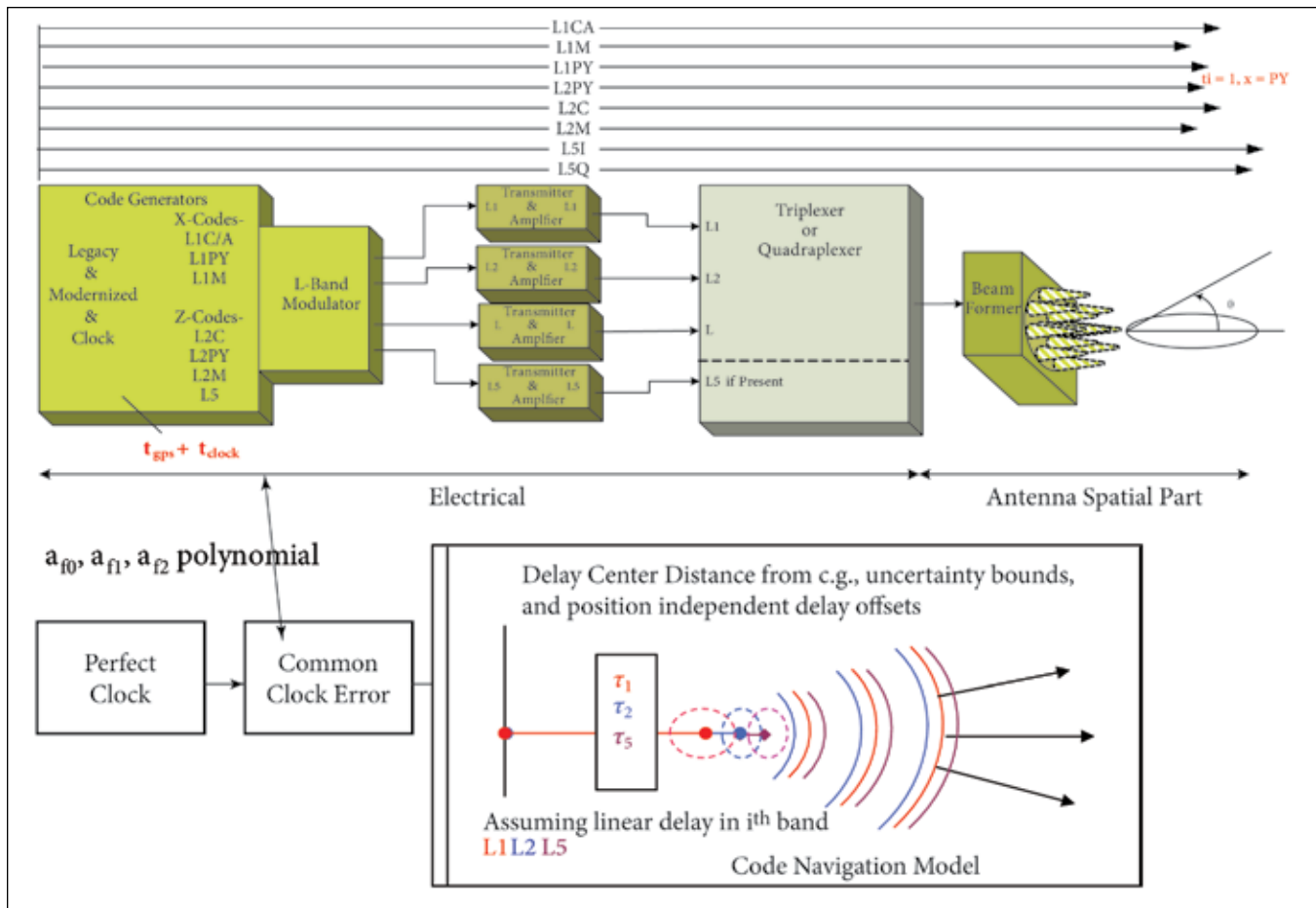
FIGURE 10 Interpreting the ISC spatial and electrical terms shown in IS-GPS-200, sections 3.3.1.7 and 30.3.3.3.1.1.1. Under small angle approximation and close delay center spacing, T_{GD}-$ISC_{Li,x}$ aligns all signals to the L1/L2P(Y) ionosphere-free ephemeris.

$$\frac{A}{f_{L1}^2} = \frac{\rho_{m_{L1,PY}} - \rho_{m_{L2,PY}} + c \bullet (ISC_{L1,PY} - ISC_{L2,PY})}{(1-\gamma)} = \qquad (18)$$

$$= \frac{[\rho_{m_{L1,PY}} - c \bullet (T_{GD})] - [\rho_{m_{L2,PY}} - c \bullet (\gamma T_{GD})]}{(1-\gamma)} =$$

$$= \frac{\rho_{m_{L1,PY}} - \rho_{m_{L2,PY}}}{(1-\gamma)} - c \bullet T_{GD}$$

because $ISC_{L1P(Y)}$=0 and $ISC_{L2P(Y)}$=(1-γ)·T_{GD}.

Although some creative book-keeping could be employed to allow the published equations to be useable, it is far better to start with a proper model of the pseudoranges that explicitly accounts for the hidden L1P(Y)-L2P(Y) term in a_{f0}. We will address that task next.

Interpreting the Modernized SV Model and Ionosphere Correction Equations

In data published in an article by C. Choi (see Additional Resources) on a prototype IIF antenna showed that distinct spatially located phase centers exist for each L-band. So, in as much as the ISCs contain delays due to electrical and antenna terms, the delays for each signal on each L-band, $\tau_{Li,x}$, contain both an electrical and antenna lever arm term.

Our full article discusses the need for measuring group delay centers, but for now we can settle on using phase center data to illustrate our point about how to interpret the a_{f0} term absorbing the L1P(Y)-L2P(Y) ionosphere-free SV equipment delay error). Because distinct phase centers exist, the actual SV equipment–delay error reflects the electrical errors and spatial lever arms to the different L-band group delay centers as pictured in **Figure 10**.

The bottom of Figure 10 shows that the effective SV equipment model has a common clock error followed by distinct delay offsets for each signal in each L-band and then up to three lever arms: an L1, L2, and, if present, an L5 lever arm. If the L band group delay centers are reasonably close together, and for a properly working SV antenna that does not impart delay changes with departure angle, then for small departure angles from boresight (less than 13 degrees for ground users) the spatial lever arm terms can be approximated by a delay about boresight with respect to the total signal-in-space error budget.

Also, note that the ISC values, which contain the sum of the electrical plus spatial antenna lumped into a delay, will be broadcast to the user. As noted in the precise positioning error budget, for receivers that operate in the greater terrestrial sphere up to three kilometers in altitude, this requires the

$$\tau_{Li,x} - \frac{\tau_{L2,PY} - \gamma \cdot \tau_{L1,PY}}{1 - \gamma}$$

$$= -ISC_{Li,x} + T_{GD}$$

Delay Center Distance from c.g., uncertainty bounds, and position independent delay offsets
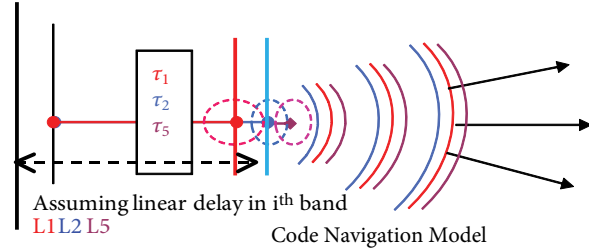
τ_1
τ_2
τ_5

Assuming linear delay in ith band
L1 L2 L5

Code Navigation Model

FIGURE 11 Interpreting the SV model: the a_{f0} offset in terms of phase/group delay center. As noted in numerous articles in the literature, the modernized SVs have unique phase centers for each L-band signal. Subtracting off the L1L2PY error term references the ephemeris equation to a location that is the linear combination of the L1PY and L2PY phase/group delay centers. That difference can be a negative number placing the ephemeris behind the SV. Under small angle approximation and close delay center spacing, T_{GD}–$ISC_{Li,x}$ aligns all signals to the L1/L2PY iono-free ephemeris

geometry to hold for up to 22 degrees off of boresight.

To interpret what it means to absorb the term

$$\frac{\tau_{L2,PY} - \gamma \cdot \tau_{L1,PY}}{1 - \gamma}$$

in Figure 5 into the a_{f0} coefficient, consider the following thought experiment. If the L1PY signal was used as the master reference signal, it would be easy to see that in Figure 5, $\tau_{L1,PY}$ is subtracted from each pseudorange; thus, a) the residual error would be $-ISC_{Li,x}$ and b) the emanation point would be the L1P(Y) delay center.

Under the small angle approximation, one can interpret the subtraction of the term

$$T_{YIFDC} \triangleq \frac{\tau_{L2,PY} - \gamma \cdot \tau_{L1,PY}}{1 - \gamma} \tag{10}$$

from all pseudoranges and its absorption into the a_{f0} term (see **Figure 11**) as placing the ephemeris of the satellite at the scaled group delay center of L2P(Y) minus γ times the delay center for L1P(Y), all scaled by (1-γ).

Thus, if the L1-minus-L2–scaled lever arms calculation produces a negative number, the ephemeris of the satellite can point to a location that is behind the satellite faceplate holding the helical array. It could be within the SV or even completely behind the SV depending on the actual values. It would still be on a line parallel to helices, piercing the satellite at the midpoint of the ring.

So, after the a_{f0} term has absorbed the L1P(Y) and L2P(Y) error, the effective SV model is that, under the small SV departure-angle approximation and with small distances between

the different L-band delay centers and a properly designed antenna, the SV acts as if there is one ephemeris for all signals by subtracting T_{GD}–$ISC_{Li,x}$ from each pseudorange.

This causes all signals to become aligned with the master L1P(Y)/L2P(Y) ionosphere-free pseudorange. Thus, the L1P(Y)/L2P(Y) ionosphere-free pseudorange is the one signal that rules all others.

Note that this is a brilliant solution to a difficult problem. If L1P(Y) were the reference, one would have to find a way to accurately remove the ionosphere. By using the L1P(Y)/L2P(Y) ionosphere-free pseudorange as the reference, as well as accepting the error of

$$T_{YIFDC} \triangleq \frac{\tau_{L2,PY} - \gamma \cdot \tau_{L1,PY}}{1 - \gamma}$$

and pulling it into the clock term, it allows one to accurately fit the clock polynomial, as long as one understands all of the physical implications.

Because everything in the satellite clock fit is referenced to the L1P(Y)/L2P(Y) ionosphere free pseudorange , this also explains why T_{GD}, an L1/L2 P(Y) term, is still needed for doing an L1/L5 correction. When looking at the modernized ionosphere-free pseudorange equation,

$$\rho_{LOS} + R_{trop} = \frac{\rho_{m_{Lj,z}} - \gamma_{ij} \cdot \rho_{m_{Li,x}} + c \cdot (ISC_{Lj,z} - \gamma_{ij} \cdot ISC_{Li,x})}{1 - \gamma_{ij}} - c \cdot T_{GD} \tag{16}$$

although the two ISC values would cover the L1 and L5 signal offsets, as noted earlier, the entire clock is fit to the L1P(Y)/L2P(Y) pseudorange. So, one must always correct from one L-band to the L1P(Y)/L2P(Y) "center point" and then proceed to the other L-band.

In the full on-line version of this article <www.insidegnss.com>, the entire model is developed from first principles and aligned with the IS-GPS-200 notation developed in Figure 20-3 of IS-GPS-200.

GPS Constellation Simulators and Receivers

Don't expect to see these effects incorporated into GPS constellation simulators any time soon. Many of the GPS constellation simulators can't easily execute these models. They may upload ISC values into the navigation messages, but they may not be able to offset the ranging codes that are on the same carrier or simulate different lever arms on the SV for each L band.

In fact, it may be useful to find out just what your GPS constellation simulator does for the L1P(Y) and L2P(Y) offset. The physical delay difference between L1P(Y) and L2P(Y) in the GPS constellation simulator hardware should be the ISC value of $ISC_{L2P(Y)}$ which is $T_{GD} \cdot (1-\gamma)$, and not T_{GD}. There ought to be separate lever arms for each L band and signal.

If simulator manufacturers are willing to use up multiple hardware channels to individually create each signal separately, then one SV out of the entire constellation could be made to have ISC effects. They could not do that for the entire constella-

tion, but for a single SV they could turn a 16-channel simulator and into a 12-channel unit and use 4 channels to simulate one SV with ISC errors for each signal.

We should also note that most GPS receivers have their own L1/L2 delay offset added to all pseudoranges due to the front-end bandpass filters. If one measures the receiver's inherent L1/L2 delay bias, it can be entered as a parameter to eliminate a clock bias that occurs when all satellite signals go through the receiver's common front-end.

However, when using a simulator, there is no receiver antenna group delay, so one will need two sets of delay constants for the receiver, with and without the receiver's antenna. Some day in the future, GPS simulators might include a true lever-arm effect and also include a right hand circularly polarized (RHCP) antenna polarization model.

Conclusions and Future Work

In this article, we derived the modernized ionosphere-free pseudorange algorithm. This was done by explicitly showing that when the L1P(Y)/L2P(Y) ionosphere-free pseudorange with the inherent SV equipment delay errors is used to calculate the final clock polynomial, moving the term

$$T_{YIFDC} = \frac{\tau_{L2,PY} - \gamma \bullet \tau_{L1,PY}}{1 - \gamma}$$

into the a_{f0} term causes the user's effective pseudorange model to become:

$$\rho_{m_{Li,x}} = \rho_{LOS} + c \bullet (T_{GD} - ISC_{Li,x}) + \frac{A}{f_{Li}^2} + R_{trop} \qquad (12)$$

By applying this model, all alternative ionosphere algorithms can then be properly modernized. We have also explained why the SV ephemeris location can be behind the SVs

As for future work, the ISCs have many other interesting aspects. For example, IS-GPS-200 talks about "the phase center" when in reality, there are multiple phase centers. In addition to accounting for multiple antenna phase centers, it also seems that the antenna's group delay and antenna group delay center ought to be used for a code-ranging model, and the antenna phase center should be used for a carrier-ranging model.

It will also be interesting to see how precise ephemeris sites such as that of the National Geospatial-Intelligence Agency <http://earth-info.nga.mil/GandG/sathtml/ephemeris.html> deal with the multiple phase centers and if the clock polynomials account for delay offsets.

Finally, additional issues emerge concerning how to measure the ISCs: for instance, should a 10 to 90 percent rise time or correlation model based on the optimal delay estimator be used? All of these questions are being studied by a team of Draper and MITRE researchers.

Additional Resources

[1] Choi, C., "Phase Centers of GPS IIF Modernization L-Band Antenna," *Proceedings of ION GPS 2002,* 24-27 September 24–27, 2002, Portland, Oregon, USA

[2] IEEE Antenna Model, IEEE Std 145-1993 (R2004), 1993

[3] IS-GPS-200 March 2006 Rev D (also in 2004 version)
a) page 17, paragraph 3.3.1.7, defining equipment group delay from frequency source to antenna phase center, but not defining antenna phase center to be for all L-bands or only one L-band.
b) page 88, 20.3.3.3.3.1 – User Algorithm for SV Clock Correction. Of particular interest: "The polynomial defined in the following allows the user to determine the effective SV PRN code phase offset referenced to the phase center of the antennas . . . ," but not indicating if it is the L1, L2, or L5 phase center.
c) page 90, 20.3.3.3.3.2. L1 – L2 correction and the definition of T_{GD}
d) page 99, 20.3.3.4.3.2. Parameter sensitivity of antenna phase center
e) page 169, 30.3.3.3.1.1.1. Inter-Signal Group Delay Differential Correction, and page 170, 30.3.3.3.1.1.2. L1/L2 ionospheric correction for L1C/A and L2C SV manufacturers will supply these values, definitions of ISC and equipment delay.
f) Definition of the inter-signal corrections (ISCs)

[4] IS-GPS-705, 20.3.3.3.2.5 has the L1/L5 modernized dual-frequency correction.

[5] Kaplan, E., and C. Hegarty, *"Understanding GPS Principles and Applications",* Second Edition, Artech House, 2006, (page 313, 7.23 and page 309 for group delay versus phase delay)

[6] Kraus, J., *Antennas,* Second Edition, McGraw Hill, 1988

[7] Mader, G., and F. Czopek, *GPS World,* "The Block IIA Satellite, Calibrating Antenna Phase Centers," May 2002

[7] Misra, P., and P. Enge, *GPS Signals, Measurements, and Performance, S8cond Edition,* Ganga-Jamuna Press, page 166, 5.30, and pages 159–160 for group delay versus phase delay.

[9] Murphy, T., and M. Harris, P. Geren, T. Pankaskie, "GPS Antenna Group Delay Variations Induced Errors in a GNSS Based Precision Approach and Landing System," Proceedings of ION-GNSS 2007, September 25–28, 2007, Forth Worth, Texas, USA

[10] U.S. Air Force, "The Precise Positioning Service (PPS) Performance Standard," <http://gps.afspc.af.mil/gpsoc/> and <http://gps.afspc.af.mil/gpsoc/gps_documentation.htm>, <http://gps.afspc.af.mil/gpsoc/documents/PPS_PS_Signed_Final_23_Feb_07.pdf>

[11] Van Graas, F., and C. Bartone and T. Arthur, "GPS Antenna Phase and Group Delay Corrections," *Proceedings of the ION National Technical Meeting 2004,* January 26-28, 2004, San Diego, California, USA

[12] Wilson, B., and C. Yinger, W. Feess, Capt. C. Shank, "New and Improved: The Broadcast Intefrequency Biases," *GPS World,* June 1999

Acknowlegments

Authors

Avram Tetewsky graduated with a master's degree in engineering from MIT 1981 and a BSEE 1976 from Rensselaer Polytechnic Institute. With C. S. Draper Laboratory since 1981, he has worked on numerous GPS-related projects including GPS simulation, spinning GPS antennas, turbulent plasma environments, and, recently, GPS modernization testing.

Jeffry Ross graduated with BSEE and MSEE degrees from Northeastern University. He has worked at the MITRE Corporation since 1995, primarily in the areas of wireless communications and navigation.

Arnold Soltz received a BA degree from John Hopkins University and an MS degree from Northeastern University. He has more than 40 years of experience in the design, implementation, and verification of the models of signals, sensors, and systems used for navigation in spacecraft, aircraft, terrestrial surveying, and undersea vehicles. He holds two Draper patents. Recent contributions have included the design and verification of a five-state Kalman filter for removing ionosphere on GPS signals.

Norman Vaughn is an engineering assistant for GPS satellite testing with Charles Stark Draper Laboratory. He graduated from the Community College of the Air Force and currently is working on his BSEE. He has 20 years of military experience in the space systems field and has worked with Draper Laboratory since 2004.

Jan Anszperger is a program manager at the Charles Stark Draper Laboratory for efforts involving GPS satellite testing and deep submergence systems. He is a graduate of Rutgers University and Florida Institute of Technology.

Chris O'Brien has 14 years' experience with RF, digital and mixed signal (including nine years at Draper), integration testing on GPS guidance systems, design of MEMS inertial instruments. He has an AAS degree in electronics and is working on a BSEE degree.

Dave Graham graduated University of Lowell and New Hampshire Technical Institute. He has 12 years of experience doing metrology, calibration, product design, and research and development at the Polaroid Corp, Waltham, Massachusetts. He is currently a senior research technician at C.S. Draper Labs.

Doug Craig is a senior member technical staff at The Charles Stark Draper Laboratory with a wide experimental background that includes building imaging radar, running an adaptive optics test lab and building fast photonic devices. His current interest is system engineering and optimizing choices in system designs. He received a master's degree and a doctorate in electrical engineering from the University of Michigan in Ann Arbor, specializing in electromagnetics and photonics.
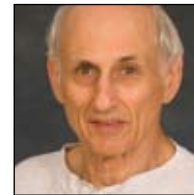
Jeff Lozow received his BSEE degree from the University of Rhode Island, an MS degree from Northeastern University, and a PhD degree from MIT. Between 1965 and 1969 he was a staff member at AVCO Missile Systems in Wilmington, Massachusetts. From 1969 to 1973 he was a member of the technical staff at the Draper Laboratory and resumed this position from 1977 until the present. His work has mainly dealt with electromagnetics, mathematical modeling, and probabilistic analysis of combined electrical and mechanical and sensor systems. **IG**

Appendices to this article are available at:
www.insidegnss.com

InsideGNSS